Rev. Fac. Ing. Univ. Antioquia N. º67 pp. 161-171, Junio, 2013

Thermally activated movement of screw dislocations in polygonized aluminum

Movimiento termo-activado de las dislocaciones helicoidales en el aluminio poligonizado

Pedro Tamayo-Meza[1], Viacheslav Yermishki[2], Juan Sandoval-Pineda[1], Luis Flores-Herrera[1], Narcizo Muñoz-Aguirre[1]*

[1]Sección de Estudios de Posgrado e Investigación, Escuela Superior de Ingeniería Mecánica y Eléctrica-UA, Instituto Politécnico Nacional. Av. de las Granjas 682, Azcapotzalco. CP 02250, México, D. F. México

[2]Baikov Institute of Metallurgy, Russian Academy of Sciences. Av. Lenninsky Prozpekt 49. 119991. Moscow, Federation of Russia.

Abstract

In this paper, we study the evolution of polygonized dislocation structures and make an analysis of plastic deformation mechanisms under creep conditions at high temperatures in polygonized aluminum of 99.3% purity. Dislocations play a role of vital importance in the evolution of plastic deformation. The influence of dislocations on the $\sigma - \varepsilon$ curve behavior as well as the shape of this curve have not yet been understood and explained. The absence of such understanding remains a problem nowadays. It is necessary to find and describe an important relationship between dislocation structures studied by means of Transmission Electron Microscopy (TEM) imag es under static conditions, the values for the yield strain, resistance to deformation, and the fracture limit. Concerning this relationship, it is relevant to mention here that the mechanical and thermal stability of defects at the sub-structural hardening drastically determines the stability of the polygonized structure under working conditions. Keeping in mind that polygonized structures are generated as a result of a thermo-mechanical treatment or directly under creep conditions, it is natural to expect that the instabilities of such structures are to be observed under much more stringent temperature and load conditions than those under which these structures were formed.

---------- *Keywords:* HVTEM, polygonization, creep, dislocations, structure, *in situ* study

* Autor de correspondencia: teléfono + 52 + 55 + 57 29 6000, ext. 64530, correo electrónico: ptamayom@ipn.mx (P. Tamayo)

Resumen

La estabilidad mecánica y térmica resultantes del endurecimiento sub-estructural en gran medida determinan la consistencia de las estructuras poligonizadas bajo condiciones de servicio. Se estudia la evolución de las estructuras dislocacionales poligonizadas y se analizan los mecanismos de deformación plástica bajo condiciones de creep a elevada temperatura en un aluminio poligonizado. El papel que juegan las dislocaciones es fundamental para el desarrollo de la deformación plástica. No ha sido fácil explicar y entender la incidencia física de las dislocaciones sobre el comportamiento y forma de la curva σ – ε, y lo realizado adoleció de una serie de problemas, y estos prosiguen hasta el día de hoy. Debía encontrarse una estrecha correlación entre la estructura dislocacional que se estudiaba mediante microscopía electrónica de transmisión, TEM, bajo condiciones estáticas, y los valores del límite de fluencia, la resistencia a la deformación y el límite de ruptura del metal. Considerando que las estructuras poligonizadas surgen como resultado del tratamiento mecánico-térmico, o directamente bajo condiciones de creep de alta temperatura, es natural esperar que la inestabilidad de las estructuras poligonizadas debe observarse bajo condiciones de temperatura y carga mucho más severas que aquellas que las generaron. El estudio de la evolución de la estructura dislocacional poligonizada del aluminio, y el análisis de los mecanismos de la deformación plástica bajo condiciones de creep a elevadas temperaturas en un aluminio poligonizado de 99,3% de pureza, es el objeto de nuestro trabajo.

---------- *Palabras Clave:* HVTEM, poligonización, creep, dislocaciones, estructura, ensayos *in situ*

Introduction

Thermal and mechanical stability of sub-structural hardness greatly determines the stability of the polygonized grain structures subject to work conditions [1, 2]. Considering the fact that polygonized structures emerge as a result of a thermo-mechanical treatment or due to creep, the changes in such structures are expected to occur under more severe conditions of force-temperature [3]. There are many publications related to creep at high temperature [4, 5]. Few of these publications report experiments *in situ* using the Transmission Electron Microscopy (TEM). In this paper, our purpose is to explain the general law of the poligonized structure behavior under creep conditions at high temperature, to understand the nature of the sources that generate free dislocations during creep, and also to explain interaction between sliding dislocations and sub-grain borders. The purpose of our experiments is to study the evolution of dislocation structures and to fulfill an analysis of plastic deformation mechanisms under creep conditions at high temperature in a pure polygonized aluminum of 99.3% purity.

The scope of our research

Dislocations are fundamental for the evolution of plastic deformation. The σ – ε curve shape depends directly on dislocations' behavior and the evolution of their movement, but such behavior has not yet been well explained. Thermo-mechanical and creep treatments play a decisive role in the process of dislocation substructure formation (in the generation of polygonized structures). It is natural to expect that the non-equilibrium of polygonized structures must be

observed under more severe temperature and load conditions than those under which they were formed [1, 2]. Therefore, in order to obtain severe temperature and load conditions over samples and to make simultaneous observations of the samples with a High Voltage Transmission Electron Microscope (HVTEM), we fabricated a special attached chamber which permitted us to study the polygonized structures' behavior under creep at high temperature, to explain the nature of the sources that generate free dislocations as well as the relationship between the sliding dislocations and the borders of the sub-grains. In this work, we discuss the results obtained *in situ* experiments.

Experimental setting

Aluminum bulk samples were previously tested in the scheme of uniaxial tension. Their original structure was obtained after an annealing treatment at *500°C* for 1 hour. The bulk samples dimensions were *50x10x0.5 mm*. Then, aluminum micro-samples were cut from the bulk samples which were previously deformed under creep conditions, and put on the TEM attached chamber. During the fabrication of the micro-samples, the stress axis was held. The shape of the micros-specimens mimicked the macro-specimens cut from a bar with sizes *5x2x0.5 mm*. Considering the electron beam of the TEM as a heating, the samples reached a stationary stage temperature in the range of 70 - 150° C°. The samples were simultaneously stressed from 25 to 32 *MPa*. The thinning of the sample was done using an oriented electrolyte flux with 10% sulfuric acid until a hole in the center of the specimen was obtained. The perforations with fine wedge shaped edges allowed transparency to electrons, where the polygonized structure was not altered under the surface image forces during the specimen preparation process. These Al structural studies under creep conditions were done *in situ* in a HVTEM, JEOL 1000, at 1000 KV. This setting allowed us to observe the dislocation behavior in thick parts of the micro-specimen, where the influence of free surfaces is negligible. The evolution of dislocation structures was recorded through a high-speed video system; likewise, the process and evolution was documented by plate photography in a periodic fashion.

Analysis of results

A typical sub-grain structure of the Al micro-specimen, prepared for *in situ* tests previous to loading, is shown in figure 1. Significant orientation is observed, the sub-grains have the shape of walls made of parallel dislocations and networks of dislocations with square and hexagonal shape, the average sub-grain size is $2.05 \pm 0.5\ \mu m$.

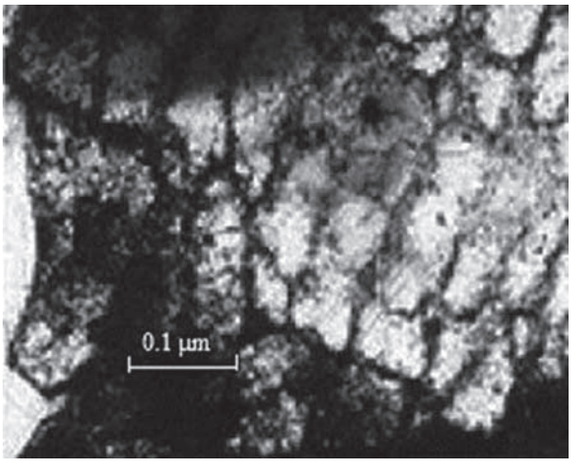

Figure 1 Sub-granular structure of polygonized aluminum

Load application moved the dislocations in which the free dislocation segments distributed in the body of the sub-grains itself started to slip first, see figure 2. During the slip, the dislocations preserve the oval loop shape corresponding to a situation where there is no significant difference between the edge and screw dislocation components. The dislocation slip occurs in systems typical for FCC crystal <110> {111}.

Figure 2 Old sub-grain boundary collapse and emergence of new sub-grain boundaries during creep in polygonized aluminum

The length of the dislocation displacement did not surpass that of the sub-grains and in an effective manner were held by the sub-boundaries. With the flow of time or when the load was increased, all of the free dislocations escaped from or were assimilated by the sub-boundaries. On the other hand, we have observed that the sub-boundaries formed early are fragmented and that the free dislocations escape from them. As a consequence, a dynamical equilibrium is established between the processes of free dislocation immobilization and the formation of new sub-boundaries with the collapse of a part of the old sub-boundaries with the generation of free dislocations as shown in figure 2.

The main characteristic of dislocations that abandon the sub-boundaries was their slipping along one of the planes of the type {111}. figure 3 shows those dislocations 1 and 2, which belong to diverse systems of the type <110> {111}, escaped and formed part of two different families of dislocations of a collapsed network in the directions shown by the arrows. Before escaping the sub-grains, the dislocations labeled 1 and 2 are straight, and as the analysis by direct visualization in the TEM (with the aid of the methods shown in [6, 7] proceeded, they were oriented 19° one from the other, had a screw character, were distributed along crystallographic directions $[21\bar{3}]$ and [011], and possessed Burgers vectors $\bar{b}_1=\pm\frac{1}{2}\,[\bar{1}01]$ and $\bar{b}_2=\pm\frac{1}{2}\,[011]$. When they leave the sub-boundary, they slip along $(111)_1$ and $(1\bar{1}1)_2$ planes.

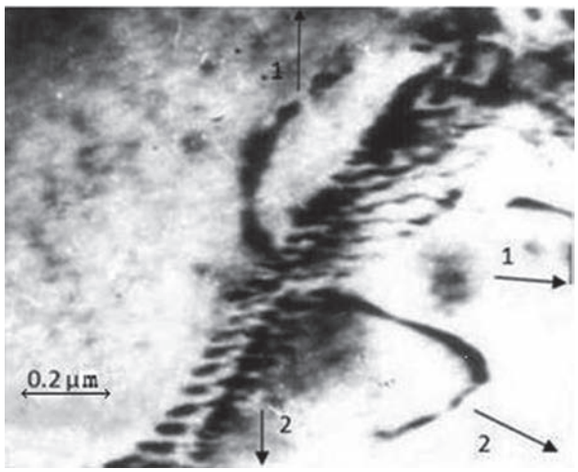

Figure 3 Dislocations escaping from the sub-grain boundaries during creep in polygonized aluminum

Such boundary structure and its behavior under load conditions are in excellent agreement with the data reported previously [7-9]. In this work we have determined not only the dislocation behavior that generates the sub-boundary, but also the sign of the Burgers vector under given orientations of the dislocation line.

To achieve this with the help of the diffraction pattern, we determined the crystallographic direction of the stress axis of the micro-specimen in the studied sub-grain and the direction of the dislocations' movement as they escaped the sub-boundary in a system of coordinates related to that sub-grain according to the next equation:

$$\bar{F}=(\bar{b}\bullet\sum)\times\bar{\zeta} \qquad (1)$$

where $\sum$ is the tensor of stresses applied to the specimen at the point where dislocations **1** and **2** are located, ζ is a unitary vector in the direction corresponding to the dislocation line. The direction of the force applied on the dislocation is thus determined as well as its projections on the plane of slip $\bar{F}_{\{111\}}$ [10]. For dislocations **1** and **2** shown in Figure 3, the stress axis of the micro-specimen coincided with the $[51\bar{3}]$ direction and the analyzed dislocations were found at the boundary of the same grain. Dislocations **1** and **2**, respectively, corresponded to the following directions: to that of their unitary vector, to the direction of the dislocation line, to the force acting upon them, and to the projection of this force on the slip plane:

$\bar{\zeta}_1 = 0.27 \bullet [21\bar{3}]$; $\quad \bar{\zeta}_1 = \frac{1}{\sqrt{2}}[21\bar{3}]$;

$\bar{F}_1 \sim [2\bar{5}, 4\bar{6}, 3\bar{2}]$; $\quad \bar{F}_2 \sim [2\bar{5}, 4\bar{6}, 4\bar{6}]$;

$\bar{F}_1 \sim (111) \sim [4\bar{5}1]$; $\quad \bar{F}_2 \sim (111) \sim [\bar{2}11]$;

In the test, the direction of their movement corresponded to the following Burgers vectors:

$\bar{b}_1 = \pm \frac{1}{2}[\bar{1}01]$; $\quad \bar{b}_2 = \pm \frac{1}{2}[011]$;

Consequently, dislocation **2**, when escaping the sub-boundary, was of a left screw character, and dislocation 1 was inclined 19° to dislocation 2, with a clear screw character. It is known that during creep, the sub-boundary formation is related to the dislocation clash and the interaction belonging to different slip systems. In our experiments, the dislocation release from sub-boundaries was related to their crossing each other and the formation of edge thresholds or jogs on them. According to, when screw dislocations of the same sign cross or dislocations with the same screw component occur, or two phenomena take place simultaneously, inter-nodal thresholds or jogs are formed. Consequently, both dislocations **1** and **2** had edge jogs of inter-nodal type. In order to determine thresholds (jogs) in dislocations **1** and **2**, it is possible to employ the following equation developed in [10]:

$$N = \frac{\left[\bar{\zeta}_1\left(\bar{r}_1 \times \bar{\zeta}_2\right)\right] \cdot \left[\bar{b}_1\left(\bar{r}_1' \times \bar{b}_2\right)\right]}{\omega\left[\bar{\zeta}_1\left(\bar{r}_1 \times \bar{\zeta}_2\right)\right]} \qquad (2)$$

This equation corresponds to the case where dislocation 1 moves towards dislocation 2. Here $\bar{r}_1$ and $\bar{r}_1'$ are the directions of the previous movement of dislocation 1 and its movement after crossing dislocation 2; ω is the atomic volume. The positive value of N corresponds to internodal jogs or thresholds and the negative N corresponds to the formation of vacancy thresholds. For dislocations 1 and 2 analyzed here, $\bar{r}_1$ and $\bar{r}_1'$ are oriented along $\tilde{F}_1$ (111) and N > 0. If dislocation 2 moved towards dislocation 1, thus reassigning indices in equation 2, $\bar{r}_2$ and $\bar{r}_2'$ are oriented along $\tilde{F}_2$ $(1\bar{1}\bar{1})$ and again N > 0. As a consequence, the verification employing the equation 2 criterion confirms the conclusions reached earlier on the formation of internodal jogs or thresholds during crossing of dislocations 1 and 2.

Discussion of results

The movement of screw dislocations with edge type thresholds or jogs, in some models of stationary creep, plays a fundamental role [10, 11]. It is supposed, that the thermo-activated movement of screw dislocations with absorption jogs or point defect birth, i.e., vacancies or interstitial atoms, are the fundamental mechanisms in the plastic deformation under stationary creep at high temperatures [12-14]. It was developed a system of equations (eqs. 3–6) that allow us to determine the stationary slip speed velocity for the screw dislocations with edge jogs or thresholds which induce movement through absorption of point defects that diffuse into them (*absorbent edges*), or through the incubation of these jogs, followed by generation by diffusion from them (*generator jogs*):

$$V_p = 4\pi \cdot D_M b^2 C_0 \left[\exp\left(\frac{A}{KT}\right) - 1\right] \qquad (3)$$

$$V_p = \frac{2\pi D_M b \lambda C_0}{\exp\left(-\frac{V_p b}{2D_M}\right) \cdot K_0\left(\frac{V_p b}{2D_M}\right)}\left[\exp\left(\frac{A}{KT}\right) - 1\right] \qquad (4)$$

For thresholds generating punctual defects and for point defect generators jogs, and

$$V_a = 4\pi D_M \cdot b^2 C_0 \left[1 - \exp\left(-\frac{A}{KT}\right)\right] \quad (5)$$

$$V_a = \frac{2\pi D_M b\lambda C_0}{\exp\left(-\frac{V_a b}{2D_M}\right) \cdot K_0\left(\frac{V_a b}{2D_M}\right)}\left[1\text{-}\exp\left(-\frac{A}{KT}\right)\right] \quad (6)$$

Equations 3 and 5 refer to the cases of non-conservative movement of the jogs and to the cases of volumetric diffusion controlled by point defects; and equations 4 and 6 describe the screw dislocation movement with jogs controlled by tubular diffusion of the point defects along the dislocation core. In equations 3–6, C_0 is the stationary concentration of point defects present in the analyzed metal under given conditions of load, temperature, etc.; D_M is the defect migration coefficient; A=0.5 x $F \cdot b$ is the work of external forces for an elementary displacement of the jog; is the mechanical force acting on the jog due to an applied stress; K is the Boltzman constant; T is temperature; $K_0\left(\frac{V_p \cdot b}{2D_M}\right)$ and $K_0\left(\frac{V_a \cdot b}{2D_M}\right)$ are Bessel modifying functions of the second degree and of the zero order. To develop equations 3–4 and determine the local concentration of point defects surrounding the jogs, an analogy was made between point defect diffusion surrounding the jogs and the heat propagation coming from a source in permanent movement inside a semi-infinite body [15], taking into account that $A = \tau \cdot b^2 \lambda$, where τ is the applied shear stress, λ is the length of the dislocation segment.

In the cases described by equations 3 and 5, a point defect source coherent with the jogs was examined as the source of point defects; for equations 4 and 6, a linear source was considered as the source of point defects, coincident with the dislocation segment. An analysis of the screw dislocations with jogs movement for fixed periods of time and their images by *in situ* HVTEM allowed an experimental determination of the majority of the parameters in equations 3 and 6. The other parameters can be calculated from known analytic formulas for specific conditions of a test. Thus, the only unknown parameter which can be calculated from equations 3 and 6 turns out to be the migration coefficient. Consequently, it is possible to use the Barrett and Nix equations for a thermo-activated analysis of the non-conservative process of the movement of the edge jogs, which control slip of the screw dislocations, and this means to decipher the physical nature of this process under real experimental conditions. In the real experimental situation in the HVTEM under an accelerating voltage above a given threshold value (200 KeV for aluminum), the result is formation of radiation defects and diffusion of point defects toward the free surfaces. This radiation damage generates a higher concentration of point defects close to dislocation jogs. This effect is equivalent to considering a higher test temperature. However, when we use equations 3 and 6, a real estimate of the point defect concentration close to the jogs was carried out starting only from the need to guarantee a defined and constant velocity of displacement of the jogs V_a (or V_p), independently of the mechanisms of formation of the point defects. No more limitations are added and hence, the analyzed equations can be used for the experimental data processing. From the sequential data recorded, and preserving the images of a selected area recorded at different times, and employing the standard analysis methods by electron microscopy, we determined the real configuration of the dislocations in their slip planes, the displacements for given time periods, and the dislocations slip systems including their Burgers vectors. Our analysis of this information allowed us to determine the dislocation velocity with jogs and the stresses acting upon them. Table 1, shows these results for one of the recorded dislocations, and in figure 4 the configuration for this dislocation is reproduced on the dislocation slip plane.

Table 1 Kinetic characteristics of slip screw dislocation with a jog

Length of dislocation travel, r·10⁶cm	54 97 125.4 199
Time t, min, of slip Velocity	45 75 105 155
V· 10⁻⁹ cm/seg	2 2.15 1.99 2.01

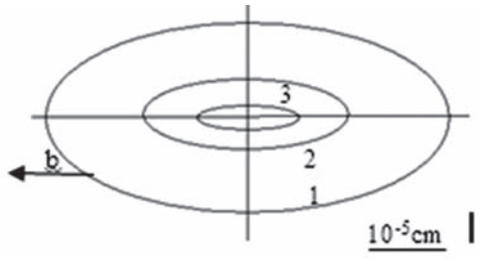

Figure 4 Calculation map for determining stress in the De Witt-Koehler approximation tress-shape diagram. The 1–3 curves correspond to the shape of the dislocation loop of Burgers vector $\bar{b}$, corresponding to a stress τ =100 (1), 200 (2) and 300 (3) kg/cm^2 [21]

These results are shown in table 1, for one of the recorded dislocations and in figure 4, the configuration for this dislocation is reproduced in the dislocation slip plane. Keeping their configuration unaltered, the dislocations in a uniform manner, slipped easily, covering a distance of 0.199 μm in 165 minutes at a speed of v~2×10^{-9}cm/seg, before the configuration was altered, as a result of its interaction with other dislocations. The shear stresses which act on the dislocations were analyzed based on the approach in [16], where the shape of the dislocation segment in the field of shear stress action was examined as an indicator of the applied stresses. On the basis of the De Witt – Koehler equations which describe the shape of the trajectory curve in the field of the shear stresses, theoretical maps of dislocation configurations were calculated for any shear stress in aluminum crystals. Calculations of the theoretical configurations of the dislocations were done in an elastic-isotropic approximation and shown in figure 4. This figure represents a diagram stress-shape. The applied shear stresses were determined by a direct comparison of a real dislocation configuration projected on its slip plane with the dislocation maps determined theoretically for different stresses. The measurement data of the geometrical characteristics of the dislocation segments was analyzed and presented in table 2 corresponding to the measurements of the shear stress. The mechanical resultant force *F*, applied on the jog in the direction of its displacement and determined by its stress τ, and the surface tension of the dislocations at their stationary position of equilibrium are is determined according to the vector sum law. The scheme to determine the resultant force, which for stationary dislocations jog movement compensates the chemical force, is shown in figure 5.

Table 2 Geometrical characteristics of slipping screw dislocations with jogs

N°. of dislocation segment	*Segment Length $\lambda \cdot 10^5$ cm*	*$\tau_i \cdot 10^{-2}$ Kg/cm^2*	*φ^0_i*	*φ^0_i*	*α^0_i*
1	1.3	2	63	57	4
2	3.4	2	21	63	11

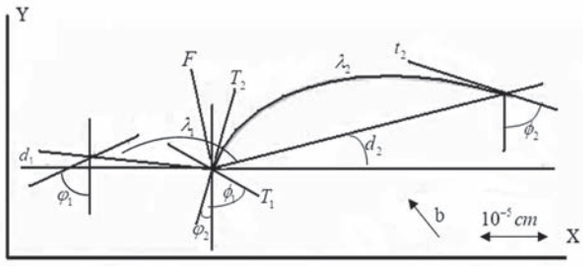

Figure 5 Scheme for the determination of the Resultant Force acting on a slipping dislocation. Two dislocation segments of lengths λ_1 and λ_2 on the slip plane X, Y, type {111}, connected with a jog and tied to the film surface. $\bar{b}$ is the Burgers vector; φ_1, φ_2, ϕ_1, ϕ_2 –angles between the linear tension stresses T_1, T_2, t_1, t_2, and the Y axis α_1, α_2 - are the angles between the lines that tie the jogs to the surface exit of the dislocation segments and the X axis; $\bar{F}$ is the force acting on the jog

According to the conventions used in figure 5, the resulting force equation can be expressed by

$$F=(T_1^2+T_2^2+2T_1 T_2 \cos\theta)^{1/2} \quad (7)$$

where the total linear stretch force is

$$T_1 = \tau \cdot b \cdot \lambda_1 \cdot \frac{\sin(\varphi_1 + \alpha_1)}{\sin(\varphi_1 + \phi_1)} \quad (8)$$

$$T_2 = \tau \cdot b \cdot \lambda_2 \cdot \frac{\sin(\phi_2 - \alpha_2)}{\sin(\phi_2 + \varphi_2)}. \quad (9)$$

The projection of the forces, determined from the equilibrium equations on the x–y axis is

$$\sum F_y = 0;\ \tau \cdot b \cdot \lambda_1 \cdot \cos\alpha_1 = t_1 \cdot \cos\varphi_1 + T_1 \cdot \cos\phi_1, \quad (10)$$

$$\sum F_x = 0;\ \tau \cdot b \cdot \lambda_1 \cdot \sin\alpha_1 = T_1 \cdot \sin\phi_1 - t_1 \cdot \sin\varphi_1 \quad (11)$$

for the segment λ_1, and

$$\tau \cdot b \cdot \lambda_2 \cdot \cos\alpha_2 = T_2 \cos\varphi_2 + t_2 \cdot \cos\phi_2, \quad (12)$$

$$\tau \cdot b \cdot \lambda_2 \cdot \sin\alpha_2 = T_2 \sin\varphi_2 + t_2 \cdot \sin\phi_2, \quad (13)$$

For the segment λ_2, T_1 and T_2 are the corresponding stretches of the dislocation segments at the point where the jog is located and t_1 and t_2 are the corresponding stretches at the points of emergence on the free surfaces of the dislocations. The definition of the angles can be observed in figure 5, and the numerical values for the analyzed dislocation are shown in table 2. The values determined for the forces for the setup of figure 5 was found to be The value for the stationary concentration of point defects was determined by [reference] as

$$C_0 = b^{-3} \cdot \exp\left[-\frac{E}{kT}\right], \quad (14)$$

where E is the energy of formation, for the corresponding defect, i.e., a vacancy or interstitial atom. For the aluminum used in this experiment E is 0.66 eV for a vacancy and 2.3 eV for an interstitial atom. The test temperature determined considering radiation effects heating was T=343°K, of the film inside the TEM at 1000 keV, and a beam current of 8 μA [17]. After substituting the parameters experimentally determined and calculated from equation 14, in equations 3–6, the migration coefficients of the point defects were calculated converging toward the jogs, or else, diverging from these, as a function of the mechanism considered as a model, that allowed the jog displacement at a constant speed determined experimentally, inside the applied stress field and at a given temperature. Furthermore, the energy activation W corresponding to the migration coefficients was determined. In our calculations we consider $D_M = D_0 \cdot \exp\left[-\frac{W}{kT}\right]$ and according to the data given in [18], D_0=1 cm²⁄sec as well as b=2.56×10^{-8}cm. In equations 4 and 6, $\lambda = \frac{\lambda_1 + \lambda_2}{2}$ and $K_0 = \left(\frac{V_{p(a)} \cdot b}{2D_M}\right) \approx \exp\left[-\frac{V_{p(a)} \cdot b}{2D_M}\right]$. The results of these calculations for the dislocation with a jog previously analyzed, shown in tables 1, 2 and figure 5, are presented in table 3 where the values expected for vacancy migration energy or for interstitial atoms are presented.

Table 3 Obtained results

Diffusion nature	*Threshold type*	*Process control*	*Dm cm²/s*	*W eV*	*H eV*	*W/ H*	*v cm/s*
Volumetric	***vacancy***	vacancy emission	1.5 e^{-22}	1.48	0.62	2.4	2.4e^{-4}
		interstitial absorption	3.1 e^{16}	*	0.1	_	2.2e^{-27}
	interstitial	emission interstitial	2.0 e^{2}	*	0.1	_	3.3e^{-13}
		vacancy absorption	2.3e^{-8}	0.52	0.62	0.84	6.7e^{-11}
Tubular	***vacancy***	vacancy emission	3.7 e^{-18}	1.19	0.19	0.3	8.6e^{8}
		interstitial absorption	2.7e^{-18}	1.26	1.26	12	2.5e^{8}
	interstitial	interstitial absorption	1.4 e^{-17}	1.14	1.14	12	4.7e^{7}
		vacancy absorption	1.2 e^{-18}	1.22	122	6.4	2.8e^{6}

* In these cases there is no physical basis to explain the obtained values for the parameters entering equations (3) and (5).

It can be clearly observed in table 3 that there is a good correlation between the energy W and H for reasonable values of the migration coefficient only for the case of dislocations' movement with thresholds interstitial, absorbed by diffusion mechanism volumetric vacancies. A direct correlation between the energy activation W for a vacancy and H for interstitial atoms for accepted values of the migration coefficient, only for the case of vacancy movement with an intermodal jog, absorbed by the volumetric diffusion of vacancies mechanism. In table 3, the values of the velocities $V_p(a)$ are shown, they were determined according to equations 3–6 using data from the references for a migration energy *H*. It is not difficult to verify that only for the case of slip of dislocations with internodal threshold, during the migration of point defects in the bulk, V_p values are obtained comparable (within an order of magnitude) with the velocities determined experimentally $V_{(p)}$ =2·10^{-9} cm ⁄sec. Here, the most acceptable values correspond to an internodal slip mechanism of the jogs, absorbing vacancies that migrate within the bulk. In all the other cases the calculated and observed values for the velocity are different by 14 – 20 orders of magnitude. The results of the present thermo-activated analysis, agree quite well with those obtained by observation in the TEM, which leads us to the conclusion that the internodal jogs formed in the dislocations escape from the sub-boundaries. Lower values of vacancy migration energy in comparison with the referenced values can be explained, from a vacancy saturation of aluminum as a result of the influence of the high energy electron flux, which under the influence of temperature at which the test was performed have sufficient mobility. If the difference in the activation energy for vacancy migration in the volume measured is:

$$C_0^i = \frac{V_a}{4\pi \cdot D_M b^2 \left[1 - \exp\left(-\frac{A}{KT}\right)\right]} \qquad (15)$$

where, in the expression for the migration coefficient , instead of the experimental activation energy W = 0.52 eV, we use the tabulated value for the vacancy activation energy for migrations 0.62 eV. The calculation according to equation 15 yields C_0^i=2.52·10^{14} b⁄cm^3.

Taking C_0^i and the equilibrium value C_0 in the absence of electron irradiation, we obtained the value for vacancy saturation in aluminum by radiation of high energy electrons:

$$\frac{C_0^i}{C_0} = \frac{2.52 \cdot 10^{14}}{8.21 \cdot 10^{12}} = 30.74, \qquad (16)$$

where in the expression for the migration coefficient instead of the experimental activation energy W = 0.52 eV, we use the tabulated value for the vacancy activation energy for migrations 0.62 eV. The calculation according to equation 15 yields C_0^i=2.52·10^{14} b⁄cm^3.

Taking C_0^i and the equilibrium value C_0 in the absence of electron irradiation, we obtained the value for vacancy saturation in aluminum by radiation of high energy electrons.

The result of $\frac{C_0^i}{C_0}$ is very similar to the conditions given at the aluminum specimen under the effect of an electron beam accelerated at 1000 kV. Consequently, as a result of the studies performed it was determined, that the collapse of the sub-boundaries under creep conditions is accompanied by the intersection of dislocations that emerge from this structure, generating jogs of inter-nodal type [18-26]. The systematic analysis of the observations of slip of screw dislocations with jogs, of edge type, demonstrated that their movement is controlled by a thermally activated displacement of the internodal jogs, realized by vacancy absorption that migrate to the jogs through the surrounding matrix. The real experimental value of the activation energy of this process is 0.52eV.

Conclusions

Observing *in situ* the images obtained by means of a high voltage Transmission Electron Microscope (HVTEM) of the evolution of the dislocation segment under sheer stress effect,

it was possible to established a directly relation between the mechanical characteristic of metal and the parameters of the dislocation structure.

During the creep process development, the sub-grain boundaries spread, and in the dislocations that abandon them jogs (thresholds) of internodal type are formed.

The analysis of the screw dislocation slip with edge jogs demonstrated, that their movement is controlled by a thermo-activated movement of the internodal jogs that occurs through migrating vacancy absorption that move towards the jogs, through the surrounding zones of the matrix.

The real experimental value of the activation energy of this process is 0.52 eV. The possible reason for this low value for the migration activation energy of vacancies in comparison with the data found in the references, resides in the fact that the aluminum matrix is saturated with vacancies induced by the electron irradiation inside the HVTEM.

Acknowledgments

The authors are grateful to Dr. Ulises Figueroa López, for fruitful discussions, to Dr. Sergey Kulagin for his help in obtaining electron micrographs in the HVTEM-JEOL 1000, the Instituto Internacional de Cooperación Técnica y Científica of SRE-México, for support during a visit to the Russian Federation (2006) and CONACyT Mexico, Project No. 84309. To *Instituto Politécnico Nacional, Escuela Superior de Ingeniería Mecánica y Eléctrica – Sección de Estudios de Posgrado e Investigación* for the provided support for this investigation.

References

1. M. Myshliayev, W. Stepanov, V. Shpeizman. “Change in creep mechanism of BCC metals”. *Phys. Status Sol. (a)*. Vol. 2. 1971. pp. 393-401.

2. M. Myshliayev, I. Jodos, O. Senkov. “Feature of the dislocation structure of grain boundaries in BCC single crystal”. *Scientific magazine titled: (FMM) Fiz. Met. Metalloved*. Vol. 48. 1979. pp. 148-151.

3. V. Rozenberg. “Fundamentals of heat resistance of metal materials”. *Scientific magazine*. Vol. 1. 1973. pp. 320.

4. K. Hale, M. Henderson. “Some applications of high voltage electron microscopy to the study of materials”. *Micron*. Vol. 1. 1970. pp. 434-464.

5. M. Myshlyaev. “Dislocation Creep”. *Annual Review of Materials Research*. Vol. 11. 1981. pp. 31-50.

6. P. Hirsh, A. Howie, R. Nicholson, D. Pashley, W. Whelan. *Electron Microscopy of Thin Crystals*. 2nd ed. Ed. R. E. Kreiger Publishing Co. Hungtington, USA. 1997.

7. M. Myshliayev, S. Olevskii, S. Maksimov. “Dislocation structure of subgrain boundaries in creep-deformed aluminium”. *Phys. Stat. Sol. (a)*. Vol. 15. 1973. pp. 391-399.

8. M. Myshliayev, D. Caillard, J. Martin. “In situ investigation of creep mechanisms of aluminum at intermediate temperatures”. *Krist. Und Technik*. Vol. 14. 1979. pp. 1325-1328.

9. J. Hirth, J. Lothe. *Theory of Dislocations*. 1st ed. Book edited by ATOMIZDAT, Moscow, USSR. 1972. pp. 599.

10. C. Barrett, W. Nix. “A model for steady state creep based on the motion of jogged screw dislocations”. *Acta Met*. Vol. 13. 1965. pp. 1247-1258.

11. W. Nix. “On the jogged screw dislocation model for steady state creep”. *Acta. Met*. Vol.15. 1967. pp. 1079-1081.

12. Y. Chadek. “Creep of Metallic Materials”. 1st ed. Book edited by MIR–11. Moscow, USSR. 1987. pp. 302.

13. V. Levitin. “The rate steady creep, Calculation and comparison with the experiments on nickel”. *Fiz. Met. Metalloved*. Vol. 32. 1971. pp. 861-870.

14. M. Wo, J. San Juan. “Structure and mobility of poligonized dislocation walls in high purity aluminium”. *Materials Science and Engineering*. Vol. 164. 1993. pp. 153-158.

15. N. Rykalin. “Calculations of thermal processes in welding”. *Mashgiz* (in Russian). Vol. 1. 1951. pp. 296.

16. G. De Wit, J. Koehler. “Interaction of dislocations with an applied stress in anisotropic crystals”. *Phys. Rev*. Vol. 116. 1959. pp. 1113-1121.

17. M. Snykers, C. Janssens, “The use of the JEM-1250 High Voltage Electron Microscope (HVTEM) of the University of Antwerp (RUCA) as an instrument for

void swelling simulation experiment". *Centre d´etude de L´energie Nucleeaire*. Report identified by: BLG-521. 1978. pp.17.

18. H. Schadler. "Mobility of edge dislocations on 110 planes in tungsten single crystals". *Act. Met.* Vol. 12. 1964. pp. 861-870.

19. I. Brodova, I. Shirinkina, T. Yablonskikha, V. Astafev*a*, E. Shorokhov, I. Zhgilev. "Structure Features of Bulk Submicrocrystalline Aluminum Alloys at High_Rate Deformation". *Bulletin of the Russian Academy of Sciences: Physics*. Vol. 73. 2009. pp. 1257-1261.

20. I. Brodova, I. Shirinkina, O. Antonova, E. Shorokhov, I. Zhgilev. "Formation of a submicrocrystalline structure upon dynamic deformation of aluminum alloys". *Materials Science and Engineering-A*. Vol. 503. 2009. pp. 103-105.

21. F. Dudaa, M. Šilhavý. "Dislocation walls in crystals under single slip". *Computer Methods in Applied Mechanics and Engineering*. Vol. 193. 2004. pp. 5385-5409.

22. H. Zhanga, L. Lia, D. Yuanb, D. Peng, "Hot deformation behavior of the new Al–Mg–Si–Cu aluminum alloy during compression at elevated temperatures". *Materials Characterization*. Vol. 58. 2007. pp. 168-173.

23. H. McQueen, N. Ryan. "Constitutive analysis in hot working". *Materials Science and Engineering: A*. Vol. 322. 2002. pp. 43-63.

24. R.Valiev, R. Islamgaliev, I. Alexandrov. "Bulk nanostructured materials from severe plastic deformation". *Progress in material sciences.* No. 45. 2000. pp. 103-189.

25. T. Lowe, L.Valiev, Z. Kluwer. "Investigations and Applications of Severe Plastic Deformation". *Proceedings of the NATO ARW*. Vol. 80. 2000. pp. 394.

26. S. Limkumnerda, J. Sethna, "Shocks and slip systems: Predictions from a mesoscale theory of continuum dislocation dynamics". *Journal of the Mechanics and Physics of Solids*. Vol. 56. 2008. pp. 1450-1459.